

# Effect of silicate layer anisotropy on cylindrical and spherical microdomain ordering in block copolymer nanocomposites

Ramanan Krishnamoorti,<sup>a)</sup> Adriana S. Silva,<sup>b)</sup> and Cynthia A. Mitchell

*Department of Chemical Engineering, University of Houston, Houston, Texas 77204-4004*

(Received 1 March 2001; accepted 24 July 2001)

The influence of the addition of small quantities of anisotropic layered silicates on the ordering of block copolymers is studied by a combination of linear viscoelasticity and small angle neutron scattering. Specifically, we examine the influence of varying the lateral dimensions of thermodynamically roughly equivalent layered silicates on the development of cylindrical and spherical microdomain order in a blend of a matched diblock and triblock copolymer. The kinetics for the development of spheres arranged on a bcc lattice from an initial disordered state are dramatically accelerated by the two larger layered silicates with equivalent diameters of  $\sim 1$  and  $10 \mu\text{m}$ , while the incorporation of an organically modified laponite, with an equivalent diameter of  $\sim 30 \text{ nm}$ , has no influence on these kinetics. On the other hand, the addition of layered silicates, irrespective of layer dimensions, has no influence on the development of cylindrical ordered microdomains and the epitaxial transformation of shear-aligned cylindrical microdomains to spherical microdomains. © 2001 American Institute of Physics. [DOI: 10.1063/1.1403004]

## INTRODUCTION

In the previous paper we reported on the ability of a highly anisotropic  $\sim 1 \text{ nm}$  thick layered silicate (organically modified montmorillonite) to influence the ordering of microphase segregated block copolymers into hexagonally packed cylinders and spheres arranged on a bcc lattice.<sup>1</sup> There we demonstrated that the silicate layers (or even tactoids of silicate layers, i.e., collections of silicate layers stacked parallel to each other) of an organically modified montmorillonite with a preferential attraction for the polystyrene block in a blend of a matched polystyrene-poly(ethylene-butene-1)-polystyrene (PS-PEB-PS) and its corresponding PS-PEB diblock copolymer,<sup>2,3</sup> was capable of templating spheres organized on a bcc lattice and dramatically enhanced the ordering kinetics of the spherical ordering from a disordered state. However, the same layered silicate had negligible influence on the cylindrical ordering of the same block copolymer system. It was suggested previously that the silicate layers were capable of organizing three-dimensional structures whose leading dimensions were much smaller than the lateral dimensions of the layers and thus were capable of templating the spherical microdomains, but not the long cylindrical microdomains. In this paper we report on the influence of the lateral dimensions of the layered silicate on the templating and mesoscopic ordering of cylindrical and spherical microdomains of a block copolymer, by comparing the kinetics of ordering for systems filled with three different layered silicates, differing essentially in terms of their lateral dimensions.<sup>2,4</sup>

The three organically modified layered silicates we have

chosen are laponite, montmorillonite and fluorohectorite with lateral dimensions of  $300 \text{ \AA}$ ,  $0.5\text{--}1.0 \mu\text{m}$  and  $10 \mu\text{m}$ , respectively. All three silicates belong to the class of 2:1 phyllosilicates or mica-type layered silicates, consisting of two silica tetrahedra sandwiching an alumina octahedron with a total layer thickness of  $9.5 \text{ \AA}$ .<sup>4,5</sup> The laponite and fluorohectorite are synthetically produced while the montmorillonite is a naturally occurring silicate, thereby resulting in higher variation in terms of the lateral size, shape, and isomorphous substitution. For all three layered silicates in consideration here, the isomorphous substitution occurs in the alumina octahedron resulting in a delocalized effective charge on the surface of the silicate layers. The laponite and montmorillonite with a charge exchange capacity (CEC) of 75 and 90 meq/100 g were modified with dimethyl-dicotadecyl ammonium chains (2C18L and 2C18M), while the fluorohectorite with a CEC of 150 meq/100 g was modified with a trimethyl-octadecyl ammonium (C18F), rendering all the organically modified layered silicates to be roughly thermodynamically equal in the context of the mean-field theory of Vaia and the self-consistent theory of Balazs and co-workers.<sup>2,6,7</sup> The isomorphous substitution of the alumina octahedra and the balancing of the charges by the ammonium head groups renders the silicate layers with a finite Lewis acid/Lewis base character, allowing for a favorable interaction with the slightly polar PS and unfavorable with the purely dispersive PEB block. In this paper, we demonstrate that while the larger silicate layers (C18F and 2C18M) accelerate the development of unaligned spherical microdomains from an initially disordered state, the addition of an equivalent amount of the smaller layered silicate (2C18L) has practically no effect on the development of the spherical microdomains. However, as previously shown, the addition of layered silicates has a negligible effect on the development of cylinders from an initial

<sup>b)</sup>Present address: Corporate R&D, Materials Sciences, The Dow Chemical Company, Freeport, Texas 77541.

<sup>a)</sup>Author to whom correspondence should be addressed. Electronic mail: ramanan@mail.uh.edu

disordered state or of bcc spheres from shear-oriented cylinders.

## EXPERIMENT

The block copolymer studied here is a blend of a triblock copolymer [polystyrene (PS)–poly(ethylene-co-butene-1) (PEB)–polystyrene (PS)] and its matched diblock copolymer (PS–PEB) (Kraton G 1657 from Shell Chemical Co., used as received). The molecular weight and microstructure characterization, phase behavior, morphology, and linear viscoelastic behavior along with the characterization of the order–order (cylinder to sphere) and order–disorder (sphere to disorder) transitions have been reported previously.<sup>1,8–11</sup> Morphologically, the unfilled block copolymer forms cylindrical microdomains of PS in a matrix of PEB below  $T_{OOT}$  ( $=138 \pm 3$  °C), with a diameter of  $\sim 27$  nm and several microns long. At temperatures above the OOT, the block copolymer forms spherical microdomains of PS with a diameter of  $\sim 23$  nm arranged on a bcc lattice. At higher temperatures, the block copolymer blend disorders, with an order–disorder transition temperature ( $T_{ODT}$ ) of  $195 \pm 5$  °C.<sup>9,10</sup>

Three organically modified layered silicates are employed in this study: a dimethyl–dioctadecyl ammonium substituted laponite (2C18L) with a CEC of 75 meq/100 g; a dimethyl–dioctadecyl ammonium substituted montmorillonite (2C18M), with a CEC of 90 meq/100 g and characterized extensively in a previous paper,<sup>12</sup> and a trimethyl–octadecyl ammonium substituted fluorohectorite (C18F) with a CEC of 150 meq/100 g.<sup>3,13</sup> The preparation of the nanocomposites and the methods of x-ray diffraction, melt state viscoelastic measurements, transmission electron microscopy, and small angle neutron scattering are described in the previous paper.<sup>1</sup>

## RESULTS AND DISCUSSION

### Structure and dispersion of nanocomposites

The nanoscale structure of the 1 wt.% layered silicate hybrids, as examined by x-ray diffraction (Cu– $K_{\alpha}$ ), is interpreted from the results presented in Fig. 1. The C18F-based nanocomposite exhibits a well-ordered intercalated structure with a layer center-to-center distance ( $h$ ) of 3.1 nm, expanding from the pristine layer center-to-center distance ( $h_0$ ) of 2.3 nm.<sup>3</sup> On the other hand, the nanocomposites based on 2C18M and 2C18L do not exhibit a peak in the range of diffraction angles studied here, indicating poor long-range order. Higher concentration hybrids prepared with 2C18M<sup>1</sup> (and a 10% nanocomposite with 2C18L, not shown here) and transmission electron micrographs presented next, show the presence of an intercalated structure with a layer center-to-center distance of  $\sim 3.1$  nm and a large number of individual layers and small tactoids with less than five layers. Thus, we conclude that for the case of 1 wt.% 2C18M and 2C18L, the nanoscale dispersion of the layered silicate is that of a disordered intercalated state and not that of a truly exfoliated nanocomposite.

To further verify the dispersion of the silicate layers in the nanocomposite hybrids, the unstained micrographs of two hybrids containing 1 and 3 wt.% 2C18M are shown in

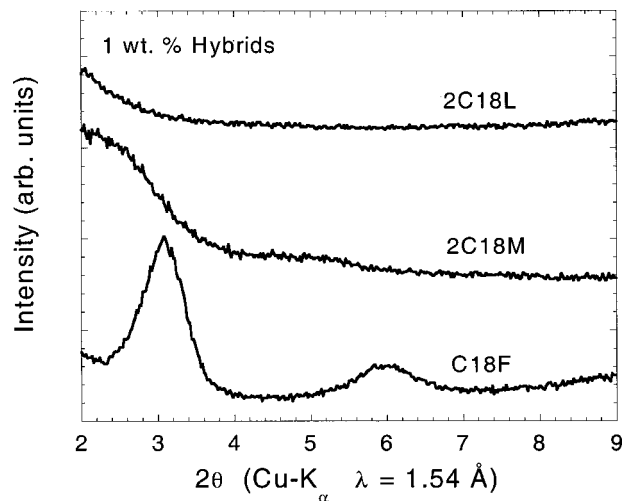


FIG. 1. X-ray diffraction spectra for the pure 2C18M and the 3 wt.% hybrid. The (001) and (002) peaks, corresponding to the midplane to midplane distance of the layered silicate, are shifted to smaller diffraction angles for the hybrid, indicating the intercalation and hence swelling of the interlayer galleries. The gallery heights were calculated using Bragg's law ( $\lambda = 1.54$  Å), the measured value of  $2\theta_{001}$ , and the known thickness of the individual silicate layers of  $\sim 9.5$  Å.

Figs. 2(a) and 2(b), respectively. The micrographs, which are representative of several tens of micrographs obtained, reveal the presence of small stacks of layers (typically less than ten layers per stack) and the frequent presence of individual lay-

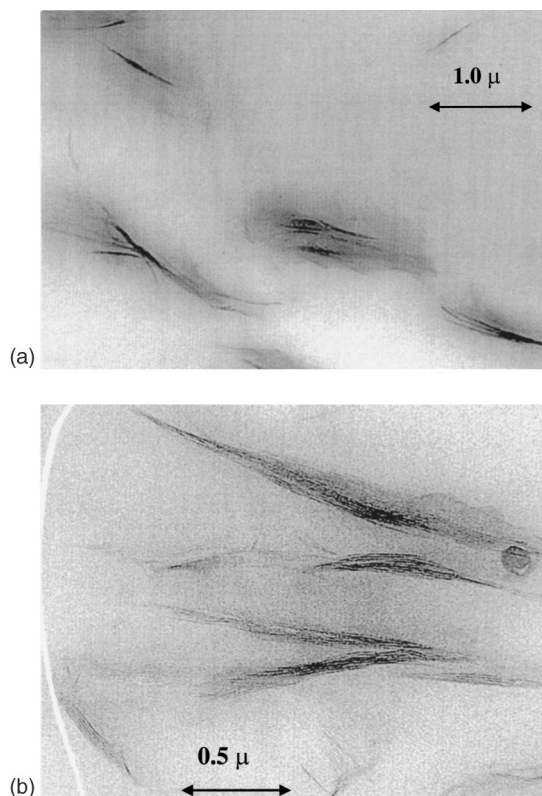


FIG. 2. Transmission electron micrographs for the 1 and 3 wt.% 2C18M hybrid [(a) and (b), respectively]. The samples were not stained and show the dispersion of the silicate layers in the polymer matrix. While stacks of the layered silicates are seen and consistent with an intercalated structure, a few individual layers are also found to be dispersed in the polymer matrix.

ers dispersed in the matrix of the polymer. In fact, previous rheological studies of polystyrene–polyisoprene block copolymer and polystyrene homopolymer-based 2C18M nanocomposites, suggested the percolation of the filler network structure for loadings as low as 5 wt.% (for 2C18M), consistent with the presence of small stacks and the frequent presence of individual silicate layers.<sup>12,14</sup>

### Ordering kinetics by linear viscoelastic measurements

The development of cylindrical and spherical order in the block copolymer blend-based nanocomposites is followed by melt-state linear viscoelastic measurements. Samples are quenched from the disordered state (typically 220 °C) to either 150 °C to obtain bcc spherical ordering, or to 120 °C to obtain cylindrical microdomain ordering. As previously described, the order–disorder transition and the order–order transition are only slightly different for the diblock, triblock, and their blend studied here,<sup>1</sup> with all three nanocomposite samples and the unfilled polymer at 120 °C, 150 °C, and 220 °C forming cylindrical microdomains, bcc spheres, and disordered states, respectively. Further, by probing the kinetics of the formation of cylindrical and spherical microdomains at identical layered silicate loading (i.e., identical levels of surface area, if fully exfoliated) and thermodynamically roughly equivalent surfaces, ensures that we can elucidate fundamental ordering behavior and the influence of flat surfaces on the development of cylindrical and spherical microdomains from such a blend of a matched diblock and triblock copolymer. The development of order is conveniently probed using low-frequency isochronal measurements, as a result of the large change in the linear viscoelastic moduli at these low frequencies during the ordering process.<sup>11</sup> In this paper, we focus on the temporal evolution of the low-frequency storage modulus as a measure of the development of microdomain order.

The kinetics for the development of bcc spherical ordering (at 150 °C), starting from an initial disordered state (at 220 °C) for the three nanocomposites with 1 wt.% layered silicate and the unfilled polymer are shown in Fig. 3. The unfilled polymer exhibits a sigmoidal growth of the modulus,<sup>15</sup> with a long incubation period and takes ~2400 min to fully develop.<sup>9–11</sup> On the other hand, the hybrids prepared with 1 wt.% 2C18M and C18F, the ordering of spherical microdomains on a bcc lattice occurs rapidly. In the preceding paper we demonstrated that for the case of 2C18M, the kinetics of growth of bcc spheres saturated beyond 1 wt.% layered silicate.<sup>1</sup> However, for the 1 wt.% 2C18L nanocomposite, the ordering kinetics appear to be unaffected by the addition of the layered silicate—the long incubation time and the sigmoidal growth are similar to that of the unfilled polymer.

On the other hand, the kinetics for the development of the cylindrical ordering (at 120 °C) starting from an initial disordered state (at 220 °C) are shown in Fig. 4 and are virtually identical for the unfilled polymer and the three nanocomposites. These results are similar to that observed previously for nanocomposites with differing levels of 2C18M incorporation, where the development of cylindrical ordering

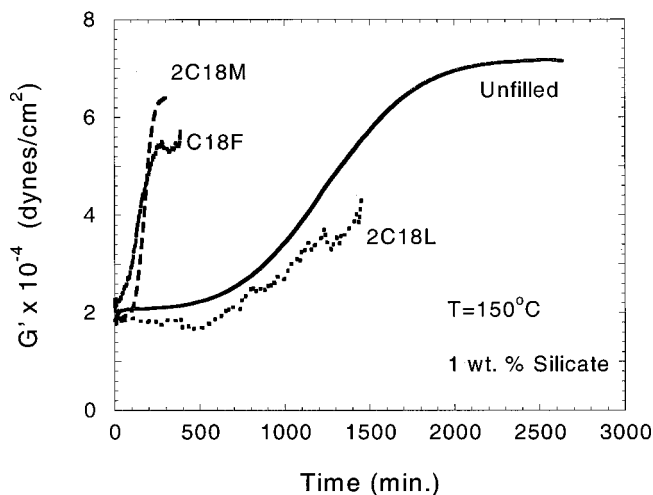


FIG. 3. Temporal evolution of the storage modulus ( $G'$ ) ( $\omega=0.03$  rad/s,  $\gamma_0=0.015$ ) for the growth of spherical microdomains at 150 °C from an initial disordered state at 220 °C for the unfilled polymer and the 1 wt.% filled hybrids. Samples are typically equilibrated thermally to within  $\pm 0.1$  °C in 10 min. Significantly enhanced ordering kinetics are observed for the C18F and 2C18M hybrids and are thought to result from the templating of the spherical microdomains by the highly anisotropic layered silicates with effective disk diameters of  $\sim 10$  and  $0.5\text{--}1$   $\mu\text{m}$ , respectively. On the other hand, the hybrid with 1 wt.% 2C18L, with a disk diameter of 30 nm and comparable to the spherical microdomain diameter, exhibits no enhancement in the ordering kinetics.

was found to be independent of silicate loading and similar to that of the unfilled polymer.<sup>1</sup>

The dramatic acceleration in the development of the spherical microdomains on a bcc lattice can be argued to result from the availability of heterogeneous nucleation sites provided by the silicate layers. However, since the silicate layers have an identical layer thickness and roughly the same physical density, the surface area per unit mass is virtually identical for all three layers ( $\sim 800$  m<sup>2</sup>/g), suggesting that the kinetics should be roughly similar for all three nanocompos-

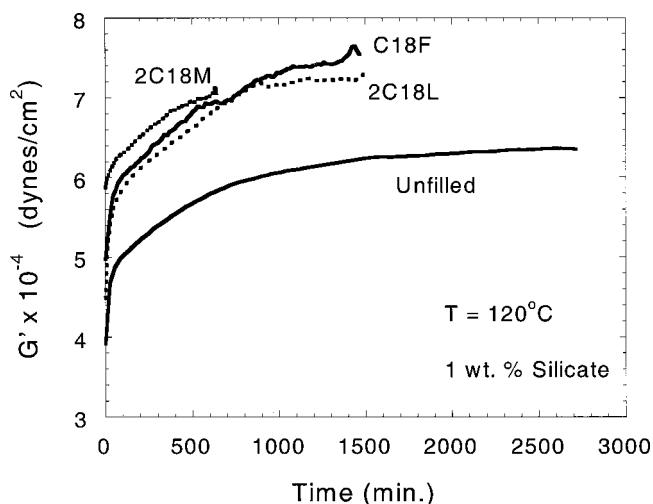


FIG. 4. Temporal evolution of the storage modulus ( $G'$ ) ( $\omega=0.01$  rad/s,  $\gamma_0=0.015$ ) for the growth of cylindrical microdomains at 120 °C from an initial disordered state at 220 °C for the unfilled polymer and the 1 wt.% filled hybrids. The kinetics for the development of cylindrical microdomains are essentially unaffected by the presence of the layered silicate.



ites. In fact, due to the higher level of layer disorder in the laponite (2C18L) based nanocomposite, as compared to the intercalated fluorohectorite (C18F) case, a larger fraction of the available silicate layer area is exposed to the polymer. Thus, if the acceleration in kinetics were exclusively a result of the presence of heterogeneous nucleation sites, it would be expected that the kinetics should be fastest for the 2C18L hybrids. Further, as argued in the Introduction, due to the similarity of the effective surface coverage by the alkyl-ammonium groups (the combination of charge exchange capacity and the length of the alkyl-ammonium tails), the thermodynamic interactions of the block copolymer with the silicate layer should be roughly similar,<sup>2,6,16</sup> implying that the thermodynamic interaction for the different layered silicates and the polymer should be similar. Thus, the accelerated kinetics for the development of spherical microdomains arranged on a bcc lattice in the presence of 2C18M and C18F cannot be attributed exclusively to the presence of heterogeneous nucleation sites.

However, it is possible that the size of the nucleating agent is crucial in determining its ability to nucleate an ordered microdomain structure. It can be argued that the 2C18M and C18F layers provide a nucleating site for the bcc spheres that is greater than the critical nucleus size, while the 2C18L layers have a size that is smaller than the critical nucleus size and hence incapable of nucleating the bcc spheres. On the other hand, all three layered silicates provide nucleating sites that are smaller than the critical nucleus size of the cylindrical microdomains. In this context, we have recently studied the ordering of a lamellar block copolymer and in that case find that for quenches close to the order-disorder temperature, the critical nucleus size decreases with increasing quench depth and is  $\sim 30$  nm for a  $1^\circ\text{C}$  quench below the ODT.<sup>17</sup>

Alternatively, for the growth and development of spherical and cylindrical microdomains it is not sufficient to have a nucleating site of a critical size. In order to generate three-dimensional ordered grains, the nucleating agent (aside from being larger than the critical nucleus size) needs to preserve and promote the symmetry of the block copolymer microdomains. In fact, it would be interesting to examine the influence of needlelike silicates such as immogilites on the development of cylindrical microdomains. Additionally, we are currently pursuing a study of the influence of layered silicates in nucleating and templating lamellar block copolymers so that we might be able to elucidate the geometrical requirements of such nanoscale nucleating agents.<sup>17</sup>

Previously, we had shown that the block copolymer blend is capable of undergoing an order-order transition from unaligned cylinders to spheres arranged on a bcc lattice with almost identical kinetics as that for the development of bcc spherical microdomains from an initial disordered state.<sup>9,11</sup> The transformation kinetics for a 1 wt.% C18F nanocomposite from an unaligned cylindrically ordered state to a spherical microdomain state arranged on a bcc lattice are compared to those for the disordered to spherical state and are shown in Fig. 5. The unaligned cylindrically ordered microdomain structure was prepared by annealing at  $120^\circ\text{C}$  for 24 h from an initial disordered state (at  $220^\circ\text{C}$ ). Consistent

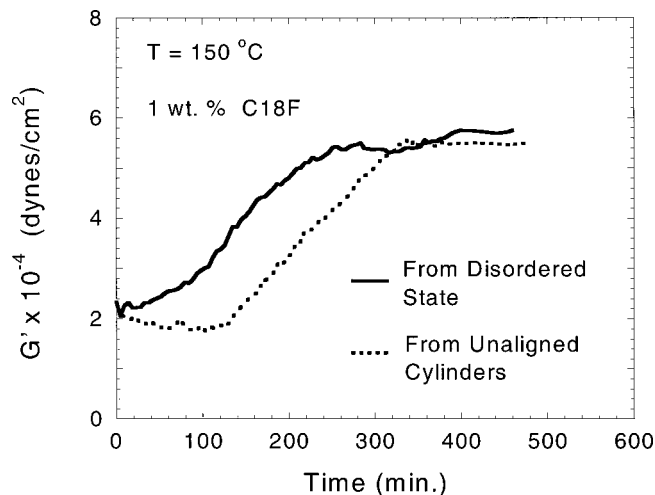


FIG. 5. The rheological signature for the development of spherical microdomains at  $150^\circ\text{C}$  from an initial disordered state (at  $220^\circ\text{C}$ ) and from a cylindrically ordered state (at  $120^\circ\text{C}$  for 24 h) for a 1 wt.% C18F filled block copolymer blend. The development of the spherically ordered state is almost independent of the initial state and is consistent with previous results on the unfilled polymer.

with the previous results for the unfilled polymer<sup>9,11</sup> and a 3 wt.% 2C18M nanocomposite,<sup>1</sup> the kinetics for the development of the spherical microdomains are nearly independent of the initial state chosen, with, in fact, a possible slowing down of the kinetics starting from an initial unaligned cylindrically ordered state.

On the other hand, starting from shear-aligned cylinders, the development of spherical microdomains on a bcc lattice occurs rapidly.<sup>9,10</sup> In the previous paper we demonstrated that these kinetics measured by rheology were unaffected by the addition of the layered silicate. We suggest that the silicate layers play no perceptible role to the development of spherical microdomains when the cylinders are well aligned and are capable of providing an original framework or scaffold from which the spheres can be developed on to a three-dimensionally arranged mesostructure. To directly probe the structural transition from shear-aligned cylinders to spheres and the effect of the dimensions of the layered silicates on this transition, we have performed SANS measurements of the order-order transition, and these are described below.

### SANS investigation of order-order transition

The two-dimensional SANS patterns with the neutron beam parallel to the velocity gradient direction for the structural transformation (under quiescent conditions) from shear-aligned cylinders (at  $130^\circ\text{C}$ ) to spheres arranged on a bcc lattice (at  $150^\circ\text{C}$ ) for a 1 wt.% C18F hybrid is shown in Fig. 6. For the shear-aligned cylinders [Fig. 6(a)], two intense spots are observed in the equatorial plane at  $q^*$ , with well-developed higher-order scattering peaks observed at  $\sqrt{3}q^*$ . The scattering signatures indicate that the sample develops well-oriented, hexagonally packed cylinders that are aligned with the cylinder axis along the velocity direction, i.e., parallel orientation.<sup>10,18</sup> On the other hand, the two-dimensional SANS pattern observed in Fig. 6(e) is consistent with that of a biaxially oriented twinned bcc spherical microdomain

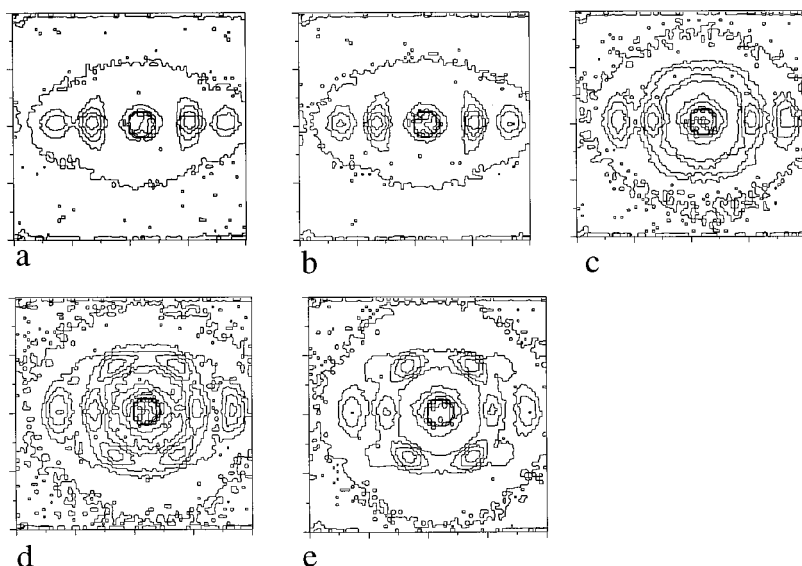


FIG. 6. Two-dimensional SANS pattern elucidating the pathway of the shear-aligned cylinder (at 130 °C) to the bcc arranged sphere transition at 150 °C for a 1 wt.% C18F nanocomposite. Panel (a) corresponds to the well-aligned cylindrical state at time=0, while panels (b)–(e) are representative patterns after 6, 17, 51, and 180 min, respectively, following the jump to 150 °C.

structure. Previously, we have shown<sup>10</sup> for the unfilled block copolymer blend, shear alignment at 150 °C leads to the development of a twinned bcc structure with primary reflections at  $q^*$  positioned at 35° to the shear direction and the higher-order reflections at  $\sqrt{2}q^*$  approximately 55° to the shear direction, consistent with the findings of Koppi *et al.*<sup>19</sup> The transformation from shear-aligned cylinders to spherical microdomains arranged on a bcc lattice in the presence of the silicate layers is consistent with the previously established epitaxial relationship between the  $\langle 001 \rangle$  axis of the cylinders and the  $\langle 111 \rangle$  axis of the spheres.<sup>19</sup>

The angular dependence of the intensity for the shear-aligned cylinder to bcc spheres in the presence of 1 wt.% C18F at 150 °C in an annular region centered on the primary peak position  $q^*$  is shown in Fig. 7. The data clearly reveal a rapid decrease in the signatures corresponding to the cylindrical structure (i.e., the peaks at 0° and 180°) and a slow increase in the intensities corresponding to the bcc structure (i.e., at 55°, 125°, 235°, and 305°). In order to compare the

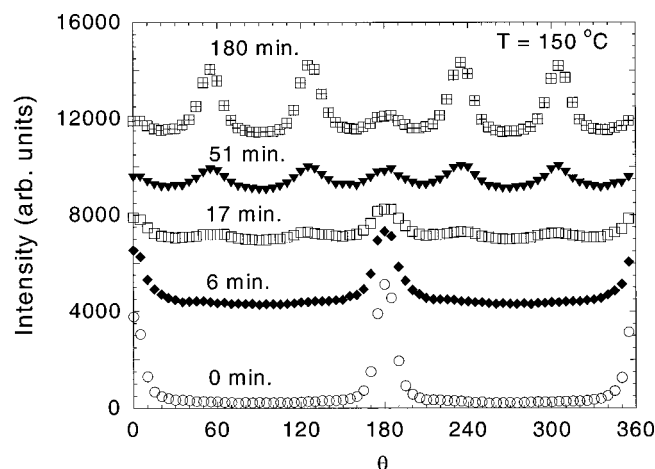
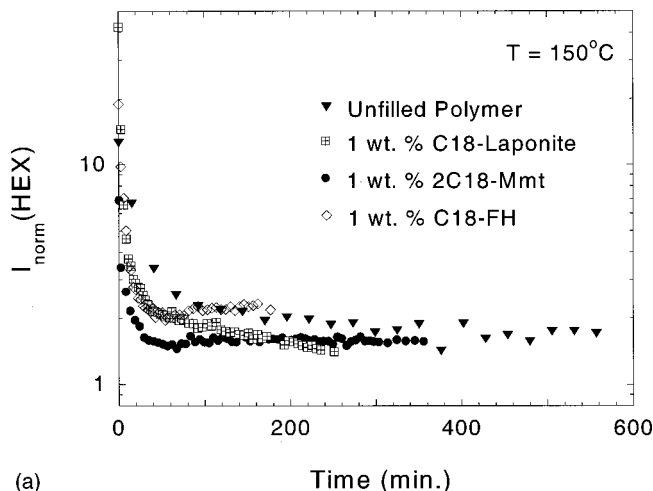


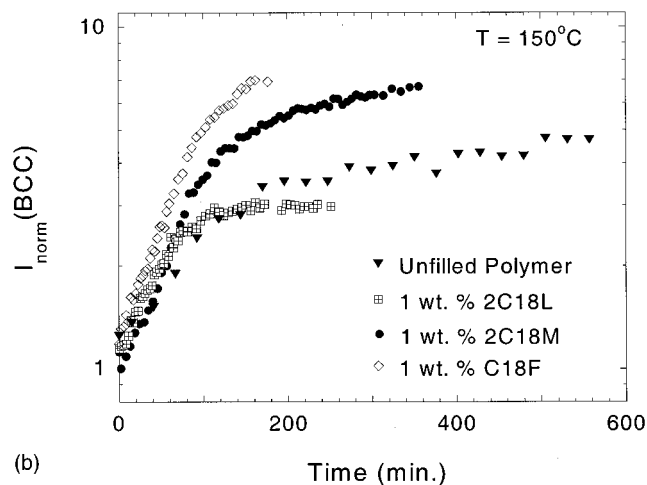
FIG. 7. The angular dependence of the SANS intensity in an annular region corresponding to  $q^*$  for the shear-aligned cylinder to sphere transition from 130 °C–150 °C for the 1 wt.% C18F nanocomposite shown in Fig. 7. The data are shifted with respect to each other to avoid overlap.

different sets of data and the time-dependent evolution of the cylindrical and spherical structure (called HEX and bcc henceforth), we normalize the average intensities corresponding to the two sets of signatures to the average of the intensities at 90° and 180°, which remain roughly invariant throughout the transformation (changing a maximum of 20% in a nonsystematic manner). The temporal evolution of these normalized intensities for the unfilled and the three nanocomposites with 1 wt.% 2C18L, 2C18M, and C18F at 150 °C from an initial shear-aligned state at 130 °C are shown in Fig. 8. We note that, as in the case of the unfilled polymer case,<sup>10</sup> the temporal evolution of the intensities for the second-order peak are similar to that of the primary peak in the case for the nanocomposites and are not shown here. These data demonstrate that the intensities corresponding to the cylindrical microdomains diminish rapidly, while those corresponding to the spherical microdomains gradually increase. Further, the kinetics of both processes are *unaffected* by the presence of the layered silicates, although for the two larger layered silicates the normalized intensities of the final spherical state are higher than that of the unfilled and the 2C18L filled polymer. It is conceivable that the larger plate diameter silicate layers leads to a better defined three-dimensional order for the spherical microdomains resulting in a higher normalized intensity for the final bcc structure. Thus, based on these SANS measurements at 150 °C, it is clear that the transformation of shear-aligned cylinders to bcc ordered spherical microdomains is unaffected by the addition of the layered silicates and is consistent with the rheological measurements reported in the previous paper.

The development of bcc ordered spherical microdomains from shear-aligned cylindrical microdomains in the unfilled block copolymer blend, reported in a previous paper,<sup>10</sup> revealed that with increasing transformation temperature, the incubation time for the development of the bcc signatures increased, and the two-dimensional pattern was roughly isotropic at intermediate times. The two-dimensional SANS data for the temporal evolution of shear-aligned cylinders to bcc ordered spheres in the presence of 1 wt.% 2C18M at



(a)



(b)

FIG. 8. The time dependence of the SANS intensity at  $q^*$  corresponding to the cylindrical microdomains and spherical microstructure for the temperature jump from 130 °C to 150 °C for the unfilled polymer and the three 1 wt.% nanocomposites. In part (a), the intensity associated with the cylindrical structure was calculated by averaging the intensities at 0° and 180° (i.e., along the equatorial plane in Fig. 7). In part (b) the intensity associated with the spherical microstructure was calculated by averaging the intensities at 55°, 125°, 235°, and 305° (i.e., 35° to the shear direction). The data for both the cylindrical and spherical microdomains were normalized by the intensity at 90° and 270°, which were roughly invariant throughout the measurement (changing roughly 20% in a nonsystematic manner).

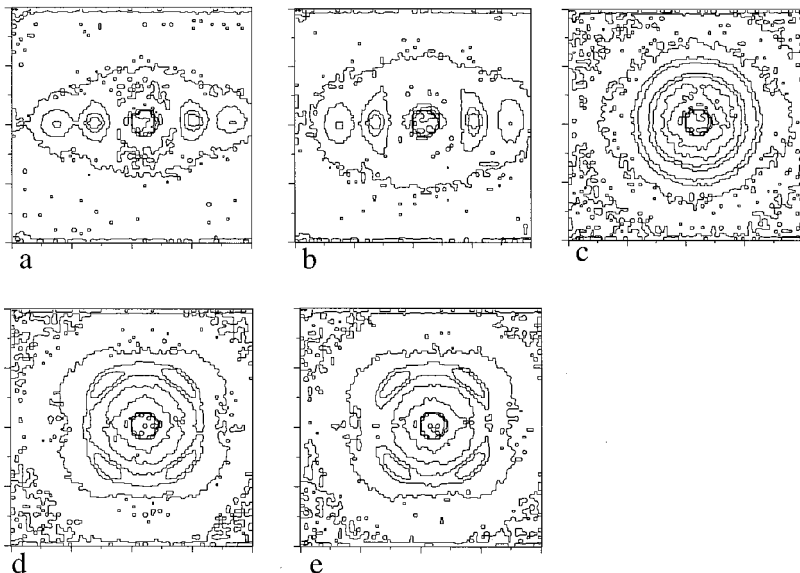


FIG. 9. A two-dimensional SANS pattern elucidating the pathway of the shear-aligned cylinder (at 130 °C) to bcc arranged sphere transition at 160 °C for a 1 wt.% 2C18M nanocomposite. Panel (a) corresponds to the well-aligned cylindrical state at time=0, while panels (b)–(e) are representative patterns after 3, 9, 115, and 255 min, respectively, following the jump to 160 °C.

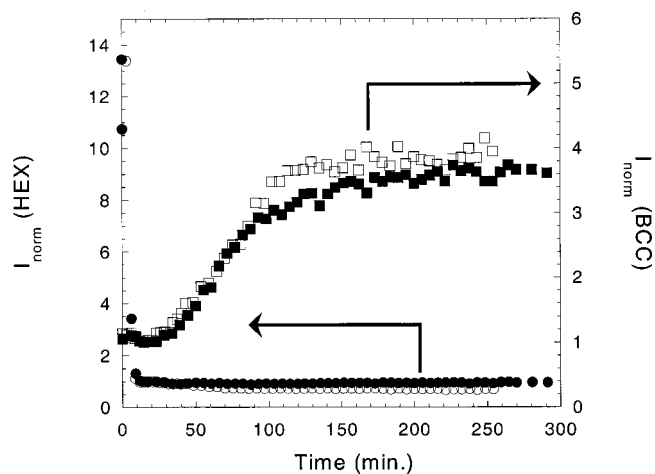


FIG. 10. The time dependence of the normalized SANS intensity at  $q^*$  corresponding to the cylindrical microdomains (circles) and spherical (squares) microstructure for the temperature jump from 130 °C to 160 °C for the unfilled polymer and the 1 wt.% 2C18M nanocomposites. The filled symbols correspond to the data for the unfilled polymer and the open symbols correspond to the data for the 1 wt.% 2C18M nanocomposite.

160 °C is shown in Fig. 9. In the presence of the silicate layer, the scattering at intermediate times becomes nearly isotropic, similar to that observed for the unfilled polymer.<sup>10</sup> However, the epitaxial relationship between the shear-aligned cylinders and the bcc spherical microdomains is preserved, as observed previously for the unfilled polymer for transformations at 160 °C and 170 °C. Quantitative comparison of the normalized HEX and bcc signatures for the transition from shear-aligned cylinders to bcc arranged spheres for the 1 wt.% 2C18M filled and unfilled polymer systems are shown in Fig. 10. The data demonstrate that the kinetics for the transformation are essentially unaffected by the presence of the silicate layers, consistent with the data obtained at 150 °C.

## CONCLUDING REMARKS

The influence of introducing thermodynamically roughly equivalent highly anisotropic layered silicates with effective

disk diameters varying from 30 nm to 10  $\mu\text{m}$  on the kinetics of ordering of a block copolymer blend to a cylindrical microdomain state and spherical microdomain state are reported here. While the kinetics for the development of randomly oriented spherical microdomains (arranged on a bcc lattice) from an initial disordered state is dramatically altered by the addition of 1 wt.% 2C18M and C18F, layered silicates with lateral dimensions of 1 and 10  $\mu\text{m}$ , respectively, the same kinetics are unaffected by the addition of 1 wt.% 2C18L with lateral dimensions of 30 nm and comparable to the size of individual spherical microdomains. On the other hand, the kinetics for the development of randomly oriented cylindrical microdomains from an initial disordered state or the epitaxial transformation of shear-aligned cylinders to bcc lattice organized spherical microdomains is unaffected by the presence of the silicate layers, irrespective of the lateral size of the layers. While it would be expected that the large surface area highly anisotropic layered silicates and the preferential attraction for the PS block would render them to be ideal candidates to be nucleation surfaces, the results presented here suggest that the layers must also provide a potential for the development of three-dimensional well-ordered structures. It is for these reasons that the silicate layers are unable to alter the kinetics for the development of cylindrical microdomains. Further, the presence of a well-defined three-dimensional ordered structure as in the case of shear-aligned cylinders leads to kinetics of shear-aligned cylinder to sphere transformation to not be affected by the addition of the layered silicates.

## ACKNOWLEDGMENTS

The authors thank J. Ren for help with the sample preparation and J. Ball for the TEM measurements. Useful discussions with Professor Giannelis, Professor Green, Professor Kumar, and Professor Manias, and Dr. Karim and Dr. Vaia are gratefully acknowledged. The authors would like to especially thank Dr. Hammouda of NIST for extensive help with the neutron scattering measurements. Funding support from the National Science Foundation (NSF) (DMR-9875321) is gratefully acknowledged. This work made use of TCSUH/MRSEC Shared Facilities supported by the State of

Texas through TCSUH and by the NSF (DMR-9632667). The SANS measurements conducted at NIST were supported by the National Science Foundation under Agreement No. DMR-9986442.

- <sup>1</sup>A. S. Silva, C. A. Mitchell, M. F. Tse, H.-C. Wang, and R. Krishnamoorti, *J. Chem. Phys.* **115**, 7166 (2001), preceding paper.
- <sup>2</sup>R. A. Vaia and E. P. Giannelis, *Macromolecules* **30**, 8000 (1997).
- <sup>3</sup>R. A. Vaia and E. P. Giannelis, *Macromolecules* **30**, 7990 (1997).
- <sup>4</sup>G. W. Brindley and G. Brown, *Crystal Structure of Clay Minerals and Their X-Ray Identification* (Mineralogical Society, London, 1980).
- <sup>5</sup>B. K. G. Theng, *The Chemistry of Clay–Organic Reactions* (Wiley, New York, 1974); B. K. G. Theng, *Formation and Properties of Clay Polymer Complexes* (Elsevier, New York, 1979).
- <sup>6</sup>A. C. Balazs, C. Singh, and E. Zhulina, *Macromolecules* **31**, 8370 (1998); A. C. Balazs, C. Singh, E. Zhulina, and Y. Lyatskaya, *Acc. Chem. Res.* **32**, 651 (1999).
- <sup>7</sup>E. P. Giannelis, R. Krishnamoorti, and E. Manias, *Adv. Polym. Sci.* **138**, 107 (1999).
- <sup>8</sup>M. F. Tse, H.-C. Wang, T. D. Shaffer, M. C. McElrath, M. A. Modi, and R. Krishnamoorti, *Polym. Eng. Sci.* **40**, 2182 (2000).
- <sup>9</sup>R. Krishnamoorti, M. A. Modi, M. F. Tse, and H.-C. Wang, *Macromolecules* **33**, 3810 (2000).
- <sup>10</sup>R. Krishnamoorti, A. S. Silva, M. A. Modi, and B. Hammouda, *Macromolecules* **33**, 3803 (2000).
- <sup>11</sup>M. A. Modi, R. Krishnamoorti, M. F. Tse, and H.-C. Wang, *Macromolecules* **32**, 4088 (1999).
- <sup>12</sup>J. Ren, A. S. Silva, and R. Krishnamoorti, *Macromolecules* **33**, 3739 (2000).
- <sup>13</sup>E. Manias, H. Chen, R. Krishnamoorti, J. Genzer, E. J. Kramer, and E. P. Giannelis, *Macromolecules* **33**, 7955 (2000).
- <sup>14</sup>C. A. Mitchell and R. Krishnamoorti, in *Polymer Nanocomposites*, American Chemical Society, Vol. 804, 2001, edited by R. Krishnamoorti and R. A. Vaia (in press); J. Ren and R. Krishnamoorti (in preparation, 2001); C. A. Mitchell and R. Krishnamoorti, *J. Polym. Sci. Part B: Polym. Phys. Ed.* (submitted, 2001).
- <sup>15</sup>J. L. Adams, D. J. Quiram, W. W. Graessley, R. A. Register, and G. A. Marchand, *Macromolecules* **29**, 2929 (1996); R. G. Larson, K. I. Winey, S. S. Patel, H. Watanabe, and R. Bruinsma, *Rheol. Acta* **32**, 245 (1993); T. Hashimoto, T. Ogawa, N. Sakamoto, M. Ichimiya, J. K. Kim, and C. D. Han, *Polymer* **39**, 1573 (1998).
- <sup>16</sup>Y. Lyatskaya and A. C. Balazs, *Macromolecules* **31**, 6676 (1998).
- <sup>17</sup>C. A. Mitchell, K. Yurekli, and R. Krishnamoorti, manuscript in preparation.
- <sup>18</sup>F. S. Bates, K. A. Koppi, M. Tirrell, K. Almdal, and K. Mortensen, *Macromolecules* **27**, 5934 (1994); M. F. Schulz, F. S. Bates, K. Almdal, and K. Mortensen, *Phys. Rev. Lett.* **73**, 86 (1994).
- <sup>19</sup>K. A. Koppi, M. Tirrell, F. S. Bates, K. Almdal, and R. H. Colby, *J. Phys. II* **2**, 1941 (1993).